Clinical Neurophysiology 145 (2023) 71–80

Contents lists available at ScienceDirect

Clinical Neurophysiology

journal homepage: www.elsevier.com/locate/clinph

Fasciculation electromechanical latency is prolonged in amyotrophic lateral sclerosis

D Planinc [a], N Muhamood [a], C Cabassi [a], R Iniesta [b], CE Shaw [a], E Hodson-Tole [c], J Bashford [a,*]

[a] UK Dementia Research Institute, Department of Basic and Clinical Neuroscience, Maurice Wohl Clinical Neuroscience Institute, Institute of Psychiatry, Psychology and Neuroscience, King's College London, United Kingdom
[b] Department of Biostatistics and Health Informatics, King's College London, United Kingdom
[c] Musculoskeletal Sciences and Sports Medicine Research Centre, Manchester Institute of Sport, Department of Life Sciences, Manchester Metropolitan University, United Kingdom

HIGHLIGHTS

- Aligned, automated outputs from muscle ultrasound and surface electromyography improved characterisation of fasciculations.
- The latency between electrical and mechanical peaks was prolonged in amyotrophic lateral sclerosis.
- Such insight into impaired excitation–contraction coupling could be translated into a novel biomarker of disease.

ARTICLE INFO

Article history:
Accepted 7 November 2022
Available online 17 November 2022

Keywords:
Fasciculation
surface EMG
ALS
Neuronal hyperexcitability
Ultrasound

ABSTRACT

Objective: In amyotrophic lateral sclerosis (ALS), motor neurons become hyperexcitable and spontaneously discharge electrical impulses causing fasciculations. These can be detected by two noninvasive methods: high-density surface electromyography (HDSEMG) and muscle ultrasonography (MUS). We combined these methods simultaneously to explore the electromechanical properties of fasciculations, seeking a novel biomarker of disease.
Methods: Twelve ALS patients and thirteen healthy participants each provided up to 24 minutes of recordings from the right biceps brachii (BB) and gastrocnemius medialis (GM). Two automated algorithms (Surface Potential Quantification Engine and a Gaussian mixture model) were applied to HDSEMG and MUS data to identify correlated electromechanical fasciculation events.
Results: We identified 4,197 correlated electromechanical fasciculation events. HDSEMG reliably detected electromechanical events up to 30 mm below the skin surface with an inverse correlation between amplitude and depth in ALS muscles. Compared to Healthy-GM muscles (mean = 79.8 ms), electromechanical latency was prolonged in ALS-GM (mean = 108.8 ms; p = 0.0458) and ALS-BB (mean = 112.0 ms; p = 0.0128) muscles. Electromechanical latency did not correlate with disease duration, symptom burden, sum muscle power score or fasciculation frequency.
Conclusions: Prolonged fasciculation electromechanical latency indicates impairment of the excitation–contraction coupling mechanism, warranting further exploration as a potential novel biomarker of disease in ALS.
Significance: This study points to an electromechanical defect within the muscles of ALS patients.

1. Introduction

Amyotrophic lateral sclerosis (ALS) is a progressive neurodegenerative disorder, characterised by the loss of upper and lower motor neurons (Longo et al., 2017). Patients present with muscle wasting and weakness, typically leading to paralysis and death within 3–5 years after symptom onset (Masrori and Van Damme, 2020). Currently, there is no cure for ALS and only one disease-

Abbreviations: ALS, amyotrophic lateral sclerosis; ALSFRS-R, ALS functional rating scale-revised; EMG, electromyography; FP, fasciculation potential; HDSEMG, high-density surface electromyography; LMN, lower motor neuron; MUS, muscle ultrasound; NEMG, needle electromyography; SPiQE, surface potential quantification engine; UMN, upper motor neuron.

* Corresponding author at: Maurice Wohl Clinical Neuroscience Institute, 5 Cutcombe Rd, London SE5 9RT, United Kingdom.
E-mail address: james.bashford@kcl.ac.uk (J Bashford).
@@SPiQEneurology (J Bashford)

https://doi.org/10.1016/j.clinph.2022.11.005
1388-2457/

modifying drug (riluzole) is licensed for use in Europe, offering only modest survival benefit (Petrov et al., 2017). There remains an urgent need for validated biomarkers to diagnose, stratify and monitor patients entering clinical trials, as the quest for effective therapies continues (Benatar et al., 2016).

Fasciculations are involuntary muscle twitches, resulting from spontaneous neuronal excitation of individual motor units (Mills, 2005). In ALS, fasciculations are an early harbinger of dysfunction as their onset typically precedes other symptoms by many months (Bashford et al., 2020c, de Carvalho et al., 2017). Two noninvasive methods have been independently employed to characterise fasciculations: high-density surface electromyography (HDSEMG) and muscle ultrasonography (MUS) (Bashford et al., 2020a, Harding et al., 2016).

HDSEMG records the summed electrical component of a fasciculation (termed *fasciculation potential*), brought about by muscle cell membrane depolarisation and repolarisation (Drost et al., 2007). The multi-channel configuration of HDSEMG enables fasciculations to be detected from a larger volume of muscle using the noise-responsive algorithm, Surface Potential Quantification Engine (SPiQE) (Bashford et al., 2019). Although this automated system identifies fasciculations with high specificity and sensitivity, it is unclear whether this surface approach is representative of the whole muscle, as the maximum depth for fasciculation detection is unknown.

MUS detects the mechanical component of a fasciculation (referred to as a *fasciculation event* where necessary) resulting from muscle fibre contraction (Bibbings et al., 2019). MUS has a high spatial resolution, capable of detecting movements as small as 5 μm (Loram et al., 2006). With regards to the diagnostic power of ultrasound-detected fasciculations in ALS, studies suggest a high sensitivity (92–96 %) and specificity (84–100 %) (Tsuji et al., 2018, Arts et al., 2012). Fasciculation detection can be quantitatively enhanced using a computational Gaussian mixture model (GMM)-based analysis approach (Bibbings et al., 2019). Moreover, recent findings suggest that ultrasound is capable of identifying movement in both the superficial and deep layers of muscle, considerably broadening the detection area surface electromyography techniques are considered to provide (Duarte et al., 2020).

In this study, we combine these two noninvasive modalities to provide unique insight into the electromechanical properties of fasciculations, anticipating that the advantages of each technique will resolve important unknowns related to the other. Relationships between depth, electrical amplitude and twitch size can be explored for the first time in this context. Uniquely, this approach produces a novel parameter that is intrinsically reliant on both modalities, specifically the time between electrical and mechanical peaks (electromechanical latency). As a direct correlate of the intramuscular excitation–contraction coupling process, this provides new insight into the pathophysiology of ALS as well as being a potential source for novel biomarker development in ALS.

2. Methods

2.1. Participants

Twelve patients, who had been diagnosed with probable or definite ALS using the revised El Escorial criteria (Brooks et al., 2000), were recruited from the King's College Hospital Motor Nerve Clinic from June 2019 to October 2019. Thirteen healthy controls were also recruited from June 2019 to December 2019 from the general population through the Manchester Metropolitan University.

Prior to the commencement of the study, we collected height, weight and age from all participants. The healthy participants undertook the RAND 36-Item Health Survey 1.0 Questionnaire (Hays et al., 1993) and the American College of Sports Medicine (ACSM) Risk Stratification Screening Questionnaire (Riebe et al., 2015). Participants were excluded from the analysis if their scores did not fall in the normal distributions for quality of life or there were significant health exclusion criteria. Healthy participants were not examined clinically. ALS participants completed the revised ALS functional rating scale (ALSFRS-R), underwent a neurological examination, and had a Medical Research Council (MRC) sum power score assessment (Cedarbaum et al., 1999, Dyck et al., 2005). Unfortunately, we only recorded regional MRC sum scores (/30 for upper limbs or lower limbs) and the total MRC sum score (/60). Although individual muscle power scores were necessarily obtained to produce these summed scores, these data were not stored individually and therefore are not available to report.

2.2. Ethical approval and consent

Ethical approval was obtained from both the local ethics committees at Manchester Metropolitan University and King's College Hospital, and the National Research Ethics Service Committee (Ref: 19/YH/0164). All participants provided informed and written consent to take part in the study.

2.3. Data acquisition

MUS and HDSEMG recordings were collected from two muscles, biceps brachii (BB) and gastrocnemius medialis (GM). The right side was chosen for investigation in both the ALS patients and healthy controls. The participants were lying relaxed on the examination couch with the arms slightly flexed and pronated and the legs slightly flexed with a slight external rotation at the hip, with the aim of making the muscles and patients as relaxed as possible. Firstly, ultrasound image sequences (depth range of 50 mm) were viewed using a linear probe (7 MHz, 59 mm long, LogicScan 128, Telemed ltd, Vilnius, Lithuania) and acoustic gel to establish the borders of the investigated muscles. The skin was then shaved if required, lightly scrubbed with a mildly abrasive gel and 70 % alcohol wipes to remove dry skin cells and skin oils to enable good electrical contact. The HDSEMG sensors were then placed on the belly of the investigated muscles and a continuous 30-minute recording was taken per muscle. Each sensor had 64 circular electrodes (8×8 grid; electrode diameter 4.5 mm; inter-electrode distance 8.5 mm; TMS International BV, The Netherlands). Reference electrodes (30×50 mm) were placed over the ipsilateral olecranon (biceps) and the patella of the knee (gastrocnemius). EMG signals were amplified by the Refa-64 EMG Recording System (TMS International BV, The Netherlands). From each channel the difference between the average signal of all the recording electrodes and the reference electrode was subtracted.

The BB muscle was assessed first, followed by GM. First, the MUS probe was manually held in place by the same operator (CC) just proximal to the HDSEMG sensor, while six 60 s MUS recordings were collected (at $\sim$ 82 frames per second; each recording separated by at least 30 s). The onsets of the MUS recordings were temporally linked to the HDSEMG trace by a rising edge of trigger output from the ultrasound device. Second, the MUS probe was moved to a position that was either lateral (for BB) or medial (for GM) to the HDSEMG sensor. A second set of six 60 s MUS recordings were then taken. As such, a total of 24 MUS recordings (12 for BB, 12 for GM), each lasting a minute, were collected per patient. During the recordings, participants were asked to remain as still and as relaxed as possible. Care was taken so that the MUS probe did not touch the HDSEMG sensor. Effort was made to ensure the transducer was parallel to the muscle fibres in longitudinal planes and perpendicular to the muscle in transverse sec-

tion, which was judged by the operator viewing the images as transducer location was established. If any excessive noise in the HDSEMG signals or any operator/participant movement was detected in the ultrasound images, that trial was discarded and repeated.

2.4. Data processing

2.4.1. HDSEMG

The signal was recorded with a sampling frequency of 2048 Hz, and both a bandpass filter (20–500 Hz) and a notch filter (50 Hz) were applied. A 64-channel sensor was used, but the electrodes on the borders (28 electrodes) were routinely excluded from analysis due to relatively poor skin contact on the periphery. Moreover, any additional faulty or compromised channels either due to poor skin contact, excessive noise, baseline drift or unexplained artefacts were excluded from analysis using specifically designed scripts (Bashford et al., 2019). Computation was performed in MATLAB (R2021a). We utilised an automated noise-responsive algorithm for identifying fasciculation potentials from raw HDSEMG data with a high classification accuracy, named Surface Potential Quantification Engine (SPiQE) and previously reported in detail (Bashford et al., 2019, Bashford et al., 2020b). In summary, it involves a spike detection mechanism based on a probabilistic analysis of spikes in relation to baseline noise and distinguishes between fasciculation potentials and voluntary movement. SPiQE thus allows for standardised comparisons between recordings taken from different patients, at different times and from different muscles. As such, fasciculation potential information such as firing time, amplitude and the channel producing the greatest amplitude were recorded.

2.4.2. Muscle ultrasound (MUS)

MUS analysis was performed in MATLAB (R2021a) using the Image Processing toolbox. To maintain objectivity of data analysis we utilised a recently proposed application of foreground detection using Gaussian mixture models (GMM), which achieved high agreement with intramuscular EMG in detecting fasciculations (82–85 % accuracy for BB and 84–90 % accuracy for MG across healthy and ALS diagnosed participants) (Bibbings et al., 2019). In summary, this approach considers fasciculation events as localised muscle tissue displacements (Pillen et al., 2008, Walker et al., 1990), resulting from electromechanical coupling. The tissue displacements are represented in image sequences as transient changes in greyscale intensity of a group of pixels localised to the region of disturbed tissue. A Gaussian mixture model is therefore constructed (based on first 500 images of a trial) and used to classify pixels as either being part of a fasciculation event, or part of the background (remaining, undisturbed tissue) (KaewTraKulPong and Bowden, 2001). For the analysis applied here, the minimum image area that should be identified as background (background ratio) was set to 90 % (healthy controls) and 80 % (ALS patients). The GMM analysis outputs a value for each image in a sequence, which is 0 in images where no fasciculation event occurred and > 0 when a fasciculation event did occur. The number and location of pixel groups identified as being part of a fasciculation event can also be extracted using this technique, providing a measure of the mean distance of the fasciculation event from the surface and hence representing fasciculation depth (Botter et al., 2021).

If there are clusters of foreground pixels in the image, they are grouped together to form a foreground object. Namely, this is when a local displacement occurred in the image, which we understand to be a MUS fasciculation event. Here, the minimum image area for pixel clusters to be classified as a fasciculation event was 20 % (healthy controls) and 10 % (ALS patients). Moreover, the mixture model for each pixel also updates when the other images are analysed. Therefore, if an intensity with a specific Gaussian model starts occurring more frequently, it becomes more highly weighted and hence describes the background. This means that the model adapts and that regular events such as blood vessel pulsation, breathing patterns and probe motions are considered as background. The learning rate of this adaptation was 0.05 (healthy controls) and 0.5 (ALS patients). All GMM parameter settings were established based on *a priori* optimisation conducted separately for ALS patient and healthy control data.

2.4.3. MUS-HDSEMG integration

The ultrasound device does not record images with a constant interval between frames, however the exact times of the frames are recorded (Miguez et al., 2017). Due to our probe's sampling rate of approximately 82 frames per second, our temporal resolution is in the region of 10–15 ms. Conversely, the duration of the whole twitch contraction averages 500 ms in duration (Walker et al., 1990).

HDSEMG fasciculation potentials were temporally aligned to MUS fasciculation events as shown in Fig. 1. A correlated electromechanical fasciculation event was identified when a MUS-detected mechanical peak (highest pixel number) occurred within a 500 ms window after the HDSEMG-detected peak amplitude (Walker et al., 1990). These correlated electromechanical fasciculation events were manually identified by two authors (DP and NM). Only recordings that were appropriately correlated and had both clear ultrasound and electrical data were included in the final analysis. Any recordings that were either lacking electrical data due to excessive noise or had poor correlation due to failure of trigger cable capturing were excluded.

Due to the mismatch between sampling rates for HDSEMG (2048 Hz) and MUS (82 Hz), we tested whether this discrepancy had any effect on the location of detected peaks. As a reduced sampling rate misses some shorter duration events, this may bias the electromechanical latency outputs between the ALS and HP groups (ALS fasciculation potentials are known to be longer due to reinnervated motor units). Fasciculation potentials from correlated electromechanical fasciculation events were rectified and down-sampled with a random start-point to 82 Hz, thereby resembling the output from MUS. The latency between the original fasciculation potential peak (at 2048 Hz) and the down-sampled fasciculation potential peak was computed. A significant deviation from zero would represent a sampling rate mismatch artefact.

2.5. Statistical analysis

Statistical analysis was performed in Prism V7.0a or R (V3.6.3). The statistical significance was set at $p < 0.05$. The Mann-Whitney test was used to identify any difference between group ages. Where there was pseudoreplication in the dataset, linear mixed-effect regression was employed in R using the *lme4* package. For all dependent variables (*depVar*) tested (e.g. latency, amplitude), the following template formula (in R notation) was used, where *muscleGroup* was the fixed effect and *participant* the random effect:

$$lmer(depVar \sim 1 + muscleGroup + (muscleGroup|participant), data)$$

QQplots were obtained to ensure sufficient adherence to the assumption of normal residuals in the model. In doing so, latency and depth were transformed by finding the square root values, whereas amplitude and pixel number were transformed by taking the $\log_{10}$ values. The model outputs a mean for the transformed variable, so although the principal dataset is not normally distributed, detransformed mean values are quoted in the results. In

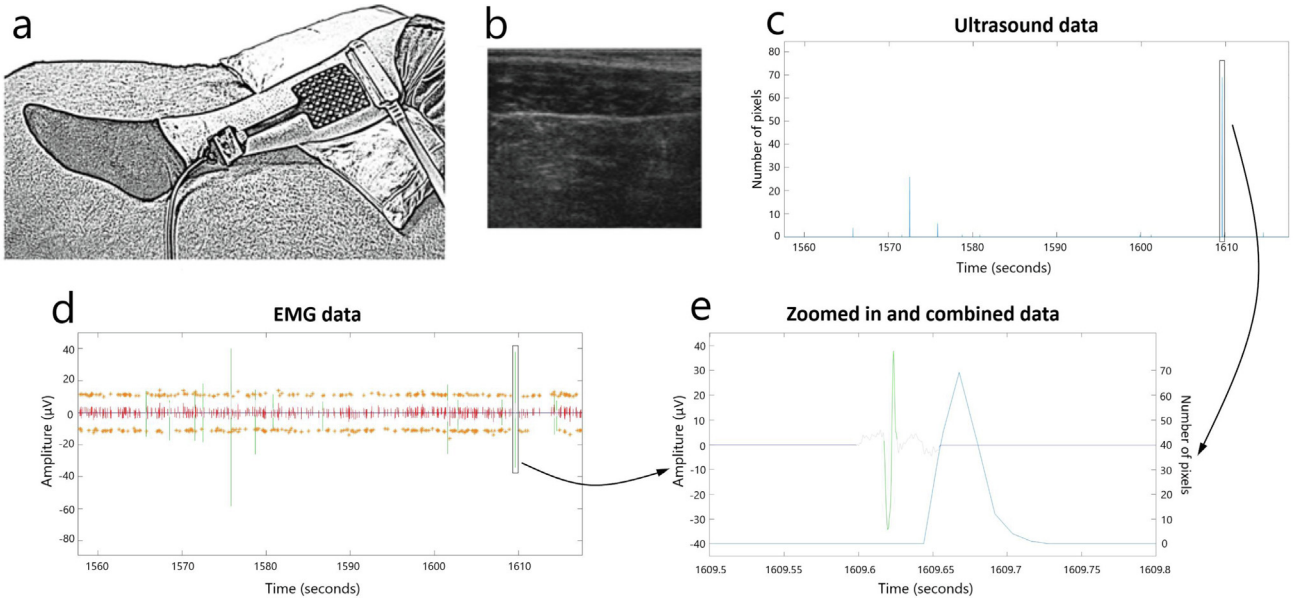

Fig. 1. Data alignment process. a) Positioning of the HDSEMG sensor and MUS probe on the leg overlying gastrocnemius medialis; b) MUS raw data; c) A Gaussian mixture model construction classified pixels as MUS fasciculation events, which are represented with blue deviations; d) Raw HDSEMG data was analysed using an automated noise-responsive spike detection mechanism (SPiQE). It distinguished between sub-threshold spikes (red) and fasciculation potentials (green). e) A zoomed in and combined section of the recording looking at the electrical (green) and mechanical (blue) components of a correlated electromechanical fasciculation event. HDSEMG = high-density surface electromyography; MUS = muscle ultrasound; SPiQE = surface potential quantification engine.

order to compute a p-value, a comparison model was run omitting the fixed effect *muscleGroup*. An analysis of variance (ANOVA) was then performed comparing the addition of the fixed effect, which produced a p-value according to the Chi-squared test. For multiple comparison testing, the *glht* function ("Generalised linear hypotheses"), which is part of the *multcomp* package (v1.4–10), was employed. Outputs from these models are reported as mean [95 % confidence interval].

For identifying relationships between parameters (e.g. depth vs amplitude), a common slope across all participants was calculated using the *rmcorr* package ("Repeated measures correlation"). Log_{10} transformations were required for the dependent variables in each comparison (amplitude or pixel number). Comparisons between electromechanical latency and clinical measures were performed by simple linear regression analysis.

3. Results

3.1. Participants

All 13 healthy controls and 12 ALS patients were included in the analysis. We analysed just over 558 minutes of aligned data. For the healthy controls, the average age was 54 (40.5–64.5) years (median [interquartile range]), height 174.5 (168–182.25) cm, weight 75 (67–88) kg, with a female to male ratio = 5:8. The RAND 36 Item Health Survey 1.0 Questionnaire revealed that their physical functioning mean score was 100 (95–100) (reference mean values for healthy participants are 70.6 ± 27.4) and their general health score was 85 (75–95) (reference mean values for healthy participants are 57.0 ± 21.1); this warranted their inclusion as healthy controls. Moreover, patients reported poor eyesight, bone/joint problems, high blood pressure, and high cholesterol as comorbid medical conditions, which were not considered contraindications for participation in this study.

ALS patient characteristics are included in Table 1. The ages of the participants did not differ between ALS and healthy cohorts (p = 0.34).

3.2. Fasciculation electromechanical latency

Median fasciculation frequencies were 25.0 per minute for the ALS-BB group, 35.0 per minute for the ALS-GM group, 6.7 per minute for the HC-BB group and 19.9 per minute for the HC-MG group. A total of 4,197 correlated electromechanical fasciculation events were identified (2,520 in ALS-GM; 1,489 in ALS-BB; 185 in Healthy-GM; 3 in Healthy-BB; Fig. 2). Due to the lack of correlated events detected, the Healthy-BB group was excluded from the statistical analysis. Compared to the Healthy-GM group (79.8 ms [60.3–100.7]; mean [95 % confidence interval]), fasciculation electromechanical latency was significantly prolonged in the ALS-BB group (112.0 ms [93.3–131.5], p = 0.0128) and the ALS-GM group (108.8 ms [78.0–142.2], p = 0.0458). There was no difference in fasciculation electromechanical latency between the two ALS muscle groups.

There was a negligible impact of down-sampling all correlated fasciculation potentials to 82 Hz (mean error for HP group = -1.0 0 ms [CI: −1.79 – −0.21 ms]; mean error for ALS group = 0.69 ms [CI: 0.49 – 0.88 ms]; *see Supplementary* Fig. 1), therefore the prolonged electromechanical latency observed was only minimally influenced by the mismatch in sampling rates between the two modalities.

3.3. Fasciculation depth, amplitude, size, and duration

Compared to the Healthy-GM group (15.0 mm [12.1–18.0]; mean [95 % confidence interval]; Fig. 3), fasciculation event depth was significantly greater in the ALS-BB group (19.2 mm [16.2–22.4], p = 0.0182) and the ALS-GM group (19.2 mm [16.8–21.7], p < 0.0001). There were no significant differences between any of the muscle groups for the amplitude or size of fasciculation events.

Compared to the Healthy-GM group (9 ms [7–10]; median [interquartile range]), fasciculation potential duration was significantly greater in the ALS-BB group (19 ms [14–28], p < 0.0001) but not significantly different to the ALS-GM group (9 ms [7–11],

Table 1
Patient characteristics. MRC = Medical Research Council; ALSFRS-R = Revised amyotrophic lateral sclerosis functional rating scale; IQR = Interquartile range. All muscle powers were assessed by the same clinician (DP).

Patient number	Age (years)	Height (cm)	Weight (kg)	Duration since symptom onset (months)	MRC sum power score (/60)	ALSFRS-R score (/48)	Gender	Site of symptom onset
1	59	173	80	26	43	44	M	Right arm
2	52	174	70	48	51	39	M	Right leg
3	67	177	65	50	58	42	M	Bulbar
4	72	175	60	71	42	41	M	Right arm
5	55	180	64	16	57	43	M	Right leg
6	63	164	75	45	42	33	F	Left arm
7	66	176	100	56	51	44	M	Left arm
8	51	170	95	24	6	29	F	Left leg
9	49	185	95	16	43	31	M	Left leg
10	48	173	75	30	56	47	M	Right arm
11	34	183	81	18	36	25	M	Right arm
12	64	164	76	9	60	46	F	Bulbar
Median (IQR)	57 (50–65)	174.5 (171.5–178.5)	75.5 (67.5–88)	28 (17–49)	47 (42–56.5)	41.5 (32–44)	Female to male ratio = 3:9	/

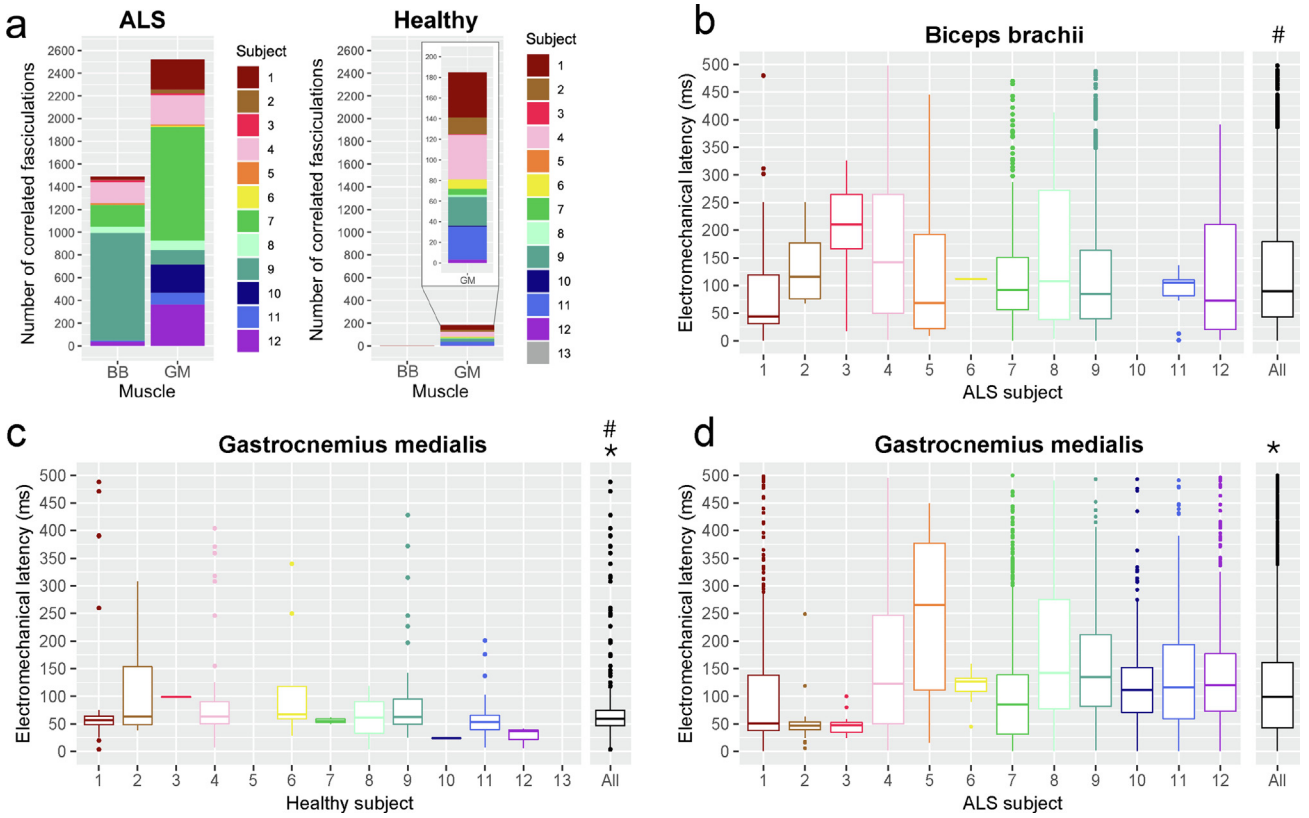

Fig. 2. Electromechanical latency. a) Number of correlated electromechanical fasciculation events detected per subject; electromechanical latency from biceps brachii (b) and gastrocnemius medialis (d) in ALS subjects; electromechanical latency from gastrocnemius medialis in healthy subjects (c). For b-d, boxes display median and inter-quartile range (IQR), and whiskers extend 1.5xIQR beyond the 1st and 3rd quartiles; outliers are identified individually. Significant group differences from linear mixed-effect regression model: #ALS-BB (mean = 112.0 ms) vs Healthy-GM (mean = 79.8 ms), p = 0.0128; *ALS-GM (mean = 108.8 ms) vs Healthy-GM (mean = 79.8 ms), p = 0.0458. ALS = amyotrophic lateral sclerosis; BB = biceps brachii; GM – gastrocnemius medialis.

p = 0.749). Median fasciculation potential duration did not correlate with fasciculation frequency for any of the groups (ALS-BB group: r^2 = 0.24, p = 0.12; ALS-GM group: r^2 = 0.01, p = 0.82; HP-GM group: r^2 = 0.16, p = 0.23).

The relationships between fasciculation potential amplitude, fasciculation event depth and fasciculation event size (reported as pixel number on MUS) according to muscle group can be found in Fig. 4 and Table 2.

3.4. MUS probe orientation

The longitudinal probe orientation detected a more uniform distribution of correlated electromechanical fasciculation events in relation to displacement from the probe (Fig. 5). In contrast, for the transverse probe position in the GM muscle, electromechanical events were disproportionately detected from the closest row of the HDSEMG grid. For the transverse position in the BB

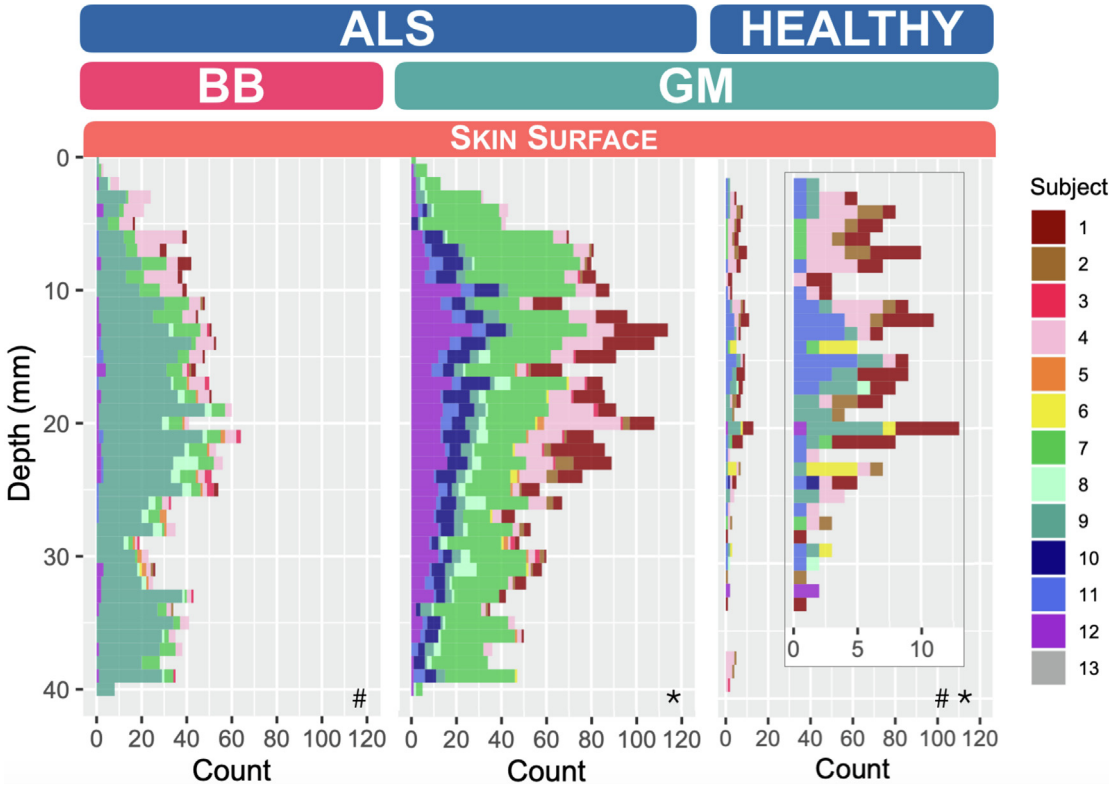

Fig. 3. Histogram of fasciculation depth from skin surface. Significant group differences from linear mixed-effect regression model: #ALS-BB (mean = 19.2 mm) vs Healthy-GM (mean = 15.0 mm), p = 0.0182; *ALS-GM (mean = 19.2 mm) vs Healthy-GM (mean = 15.0 mm), p < 0.0001. ALS = amyotrophic lateral sclerosis; BB = biceps brachii; GM = gastrocnemius medialis.

muscle, an interesting pattern was observed, whereby electromechanical events from row five on the HDSEMG grid were conspicuously lacking, consistent with the location of the innervation zone of the muscle.

3.5. Clinical markers of disease

Amongst the 12 ALS patients, fasciculation electromechanical latency did not show any significant correlations with months since symptom onset, ALSFRS-R, MRC sum score or fasciculation frequency/amplitude dispersion (Fig. 6).

4. Discussion

Through the complementary detection of the electrical and mechanical components of fasciculations, this study demonstrates a prolonged electromechanical latency in ALS muscles compared to healthy muscles. This directly indicates an impairment of the excitation–contraction coupling mechanism within ALS muscles and may contribute to the prominent muscle weakness and fatigue experienced by patients. The fact that fasciculation electromechanical latency did not correlate with disease duration, symptom burden or sum muscle power in this small, cross-sectional cohort should not discourage further evaluation as a potential biomarker of disease, particularly as part of a serial study design.

The excitation–contraction coupling mechanism in skeletal muscles involves a complex sequence of events, namely: 1) Depolarisation of the neuronal membrane at the neuromuscular junction followed by acetylcholine release from the motor neuron terminal; 2) Sodium ion influx across the muscle membrane causing depolarisation and propagation of an action potential into the muscular T-tubule system; 3) Sequential activation of the dihydropyridine CaV1.1 receptors and ryanodine receptors in the sarcoplasmic reticulum, and 4) Calcium release from the sarcoplasmic reticulum that initiates actin-myosin crosslinking and contraction, followed by calcium sequestration and muscle relaxation (Calderon et al., 2014). Although we observed a delay between the electrical peak (step 2 of the above sequence) and the mechanical zenith (step 4) in ALS muscles *(see Supplementary Video)*, our methodology is not capable of localising and characterising the causative impediment(s) in the process. Interestingly, while one study in an ALS mouse model (G93A-SOD1) showed reduced depolarisation-induced Ca^{2+} release from the sarcoplasmic reticulum attributable to dysfunction of the CaV1.1 channel (Beqollari et al., 2016), another study revealed no deficiencies in electrically evoked calcium transients (Chin et al., 2014). Therefore, although the mechanisms for our observations are unclear, the delay in contraction must point to defective propagation within skeletal muscle. Additional strategies to elucidate the underlying mechanism for prolonged EML in human subjects include assessing the impact of pharmacological intervention (e.g. with the fast skeletal muscle troponin activators tirasemtiv/reldesemtiv or the muscle sodium channel antagonist mexiletine) and evaluating the influence of motor unit twitch speed by calculating muscle fibre conduction velocity.

The influence of the neuromuscular junction on electromechanical latency remains uncertain. Increased jitter as a result of neuromuscular junction dysfunction leads to fasciculation potentials with greater variability in morphology (both amplitude and duration), but due to the relative insensitivity of surface electrodes to detect the activity of individual muscle fibres (contrast this with single-fiber needle EMG) this variability would be subtle. For jitter analysis, it is essential to record multiple muscle fibre action

Fig. 4. Correlation between fasciculation depth, amplitude and size. Please refer to Table 2 for quantitative correlations. ALS = amyotrophic lateral sclerosis; BB = biceps brachii; GM = gastrocnemius medialis.

potentials from the same motor unit, either by voluntary contraction or electrical stimulation of the nerve; neither of these were performed in this study. We do not routinely perform repetitive nerve stimulation or single-fibre EMG in our ALS patients, therefore this information is not available retrospectively for this cohort. This requires specific attention in future studies.

We found that the surface electrodes were capable of reliably identifying fasciculation potentials as deep as 3 cm. Given a surface area for the high-density surface grids of approximately 46 cm^2, this implies a volume of detection approaching 138 cm^3. This paper circumvents the issues of voluntary activity in tackling the issue of depth detection of HDSEMG as it relies on spontaneous neuromuscular events. This is novel and highlights the significant spatial accuracy not yet encountered in the literature. This is especially important, considering the correlated electromechanical fasciculation events in this study were detected further from the skin surface in ALS muscles than in healthy gastrocnemius muscles. Assuming an average skeletal muscle fibre cross-sectional diameter of 50 μm and a muscle fibre:motor unit ratio of approximately 2000 in gastrocnemius (Feinstein et al., 1955), the high-density surface grids could theoretically detect activity in up to 520 motor units, whereas needle EMG was estimated to record activity from 5-40 motor units (Mills, 2010, Daube and Rubin, 2009). Thus, HDSEMG offers a major increase in sample size over needle EMG

Table 2
Relationships between fasciculation potential amplitude and fasciculation event depth and size (pixel number) according to muscle group. HDSEMG = high-density surface electromyography; ALS = amyotrophic lateral sclerosis; BB = biceps brachii; GM = gastrocnemius medialis; r = correlation coefficient.

Muscle group	% change as fasciculation event depth increased by 10 mm		% change as fasciculation event pixel number increased by 10
	HDSEMG amplitude	Pixel number	HDSEMG amplitude
ALS-BB	−2.6 % *(r = -0.06; p = 0.0279)*	−24.5 % *(r = -0.3; p < 0.0001)*	+7.1 % *(r = 0.1; p = 0.0004)*
ALS-GM	−5.9 % *(r = -0.1; p < 0.0001)*	−25.2 % *(r = -0.3; p < 0.0001)*	+0.7 % *(r = 0.015; p = 0.448)*
Healthy-GM	−7.3 % *(r = -0.115; p = 0.131)*	+1.1 % *(r = 0.013; p = 0.87)*	−9.2 % *(r = -0.1; p = 0.188)*

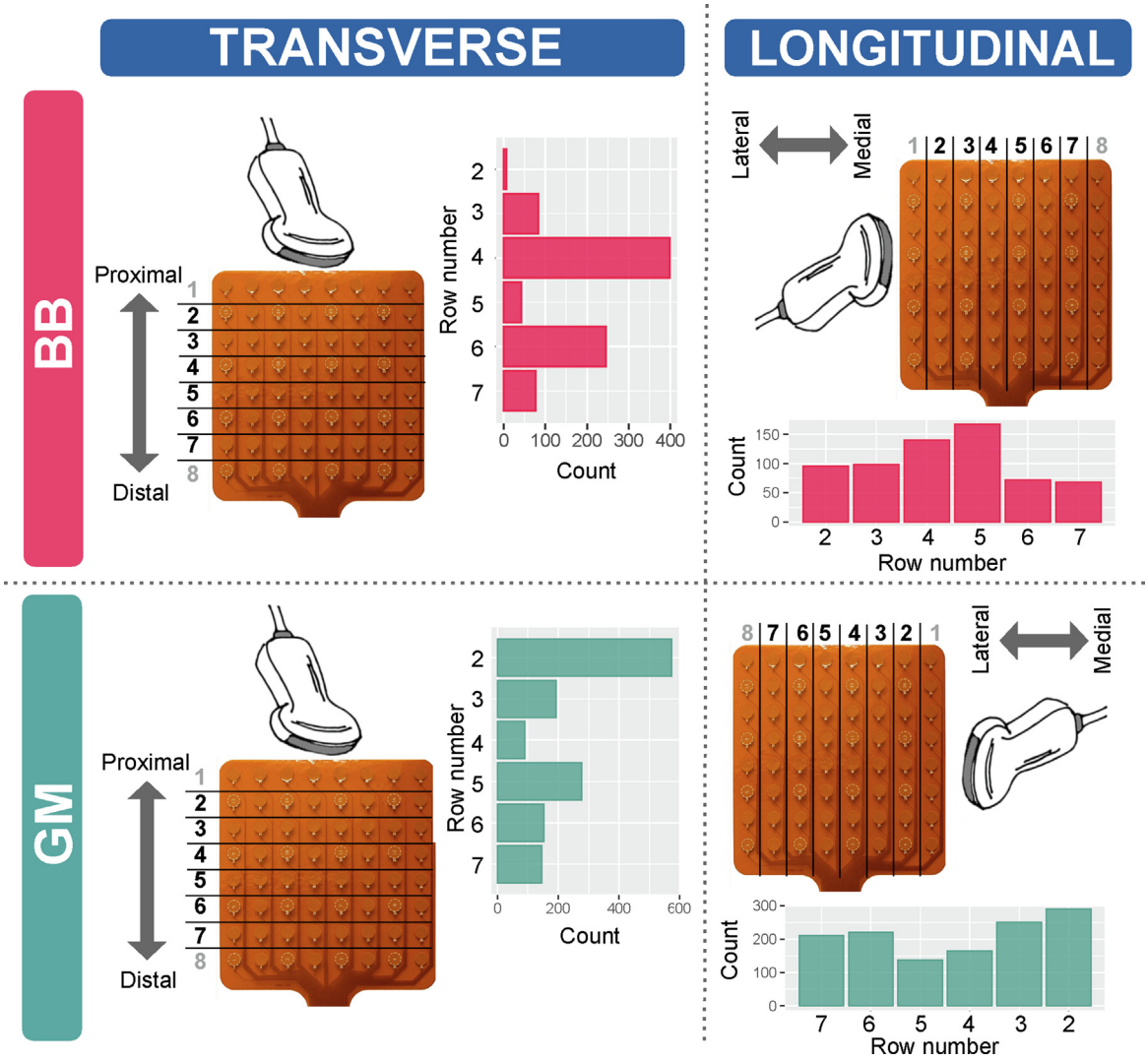

Fig. 5. Effect of row displacement on number of correlated electromechanical fasciculation events according to muscle and orientation of ultrasound probe. BB = biceps brachii; GM = gastrocnemius medialis.

despite the challenges of surface detection of intramuscular action potentials (Mesin and Farina, 2005). Additionally, the design of the electrode array and subsequent processing will impact these estimations (Botter et al., 2021).

Interestingly, we found that fasciculation depth was significantly greater in both ALS subgroups compared to healthy controls. The reason for this remains unclear and warrants further investigation. Firstly, there could be a particular propensity for slow-twitch muscle fibres, which are known to be more amenable to compensatory reinnervation in mouse models, to lie more deeply in the muscle architecture (Kaplan et al., 2014). Secondly, it is possible that fasciculations of deeper muscles (such as soleus) that are not known to fasciculate significantly in healthy individuals are detected in the ALS patients, particularly considering the likely

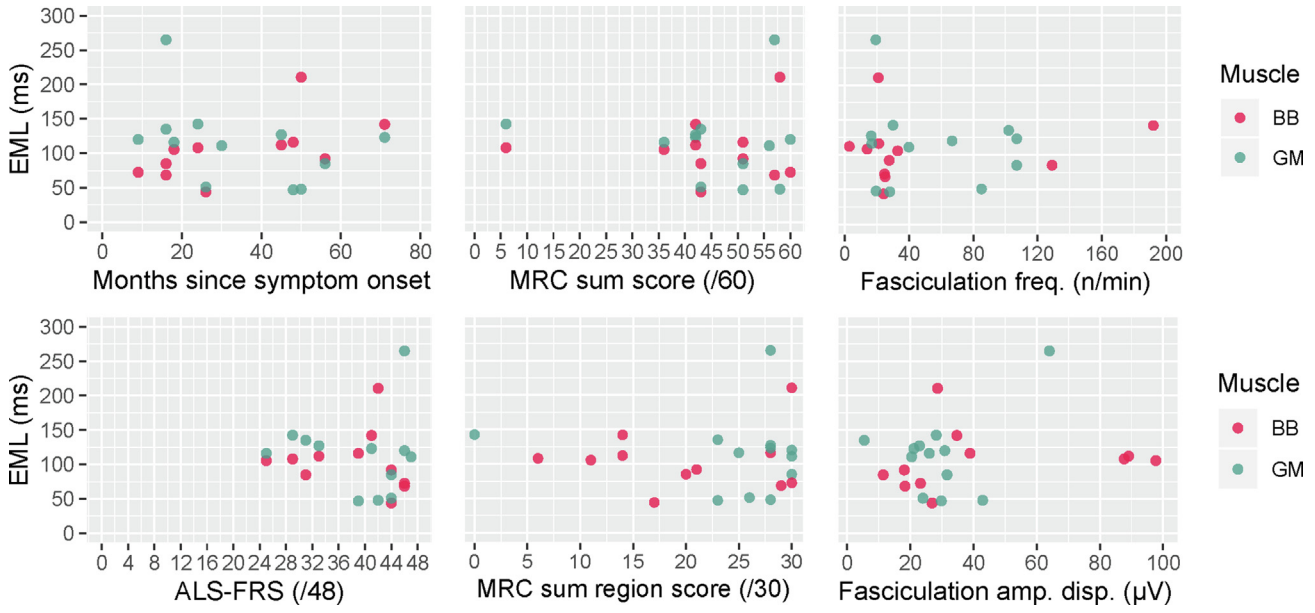

Fig. 6. Correlations between fasciculation electromechanical latency (EML) and clinical or fasciculation parameters in ALS patients. There were no significant correlations between EML and the other parameters. EML = electromechanical latency; BB = biceps brachii; GM = gastrocnemius medialis. ALSFRS-R = Revised amyotrophic lateral sclerosis functional rating scale; MRC = Medical Research Council.

atrophy of the superficial gastrocnemii. Thirdly, looking at our dataset, the ALS individuals contributing a significant number of fasciculations (Fig. 3) represent patients with a higher body mass index compared to healthy participants and perhaps this 4 mm difference could be explained by an increase in subcutaneous adipose tissue.

Although the strength of the associations was weak (|r|<0.3), HDSEMG fasciculation potential amplitude was reduced by increasing depth and decreasing size of the fasciculation event. Multiple motor unit factors influence the HDSEMG amplitude, such as distance from the electrode (following the principle of volume conduction), motor unit subtype (fast-twitch units are larger) and the extent of reinnervation (as part of the chronic partial denervation process characteristic of ALS) (Zwarts and Stegeman, 2003, de Carvalho and Swash, 2016). By additionally distinguishing motor unit subtype with the calculation of muscle fibre conduction velocity and afterhyperpolarisation (both derivable from HDSEMG grids after motor unit decomposition) (Weddell et al., 2021), greater focus on the electromechanical alterations attributable to chronic partial denervation could be achieved in future, larger studies. Furthermore, how pathophysiological myocytes may trigger, exacerbate, or even curb neurodegeneration in a non-cell autonomous fashion is an unresolved issue demanding new investigative strategies such as this (Maimon et al., 2018, Dadon-Nachym et al., 2011).

We acknowledge several limitations to this study. Only two muscles were assessed, so it is unknown how generalisable our conclusions are to other muscles, particularly the clinically relevant, smaller intrinsic hand muscles. The inherent characteristic of the ultrasound as an imaging modality implies a lack of standardisation of the recorded results and the field of view. Despite significant care with live image observation, we acknowledge that the angle between the imaging plane and muscle fibres is unlikely to be constant across participants, however, due to the connectedness of fibres within the muscle volume, displacements in muscle tissue are likely to be seen in the whole segment. Therefore, although a single plane of muscle is imaged it cannot be considered independent of the surrounding muscle structures. Fibres will lie on a path through the plane, and extracellular matrix and other connective components will connect the fibres. There might be a delay in our measurements depending on the distance between the excited fibres and imaging plane. However, this is not specific to any group (healthy vs ALS), and we do not think it would directly affect our results, particularly given the temporal resolution of the ultrasound. ALS subject 10 had a monomelic variant of motor neuron disease at the time of recording, differing from the remaining patients with a classical ALS phenotype. Correlated electromechanical fasciculation events were an order of magnitude more numerous in ALS patients compared to healthy controls, limiting the comparative ability of the analysis. Fasciculations detected by one modality but not the other were discarded from this analysis. Uncorrelated instances have been reported in previous studies of fasciculations in healthy individuals, although the reason for their occurrence is not clear (Botter et al., 2021). In the work presented here, such instances could be more common at higher fasciculation frequencies, as more than one fasciculation potential (from different motor units) may occur before the detection of the first mechanical correlate. This could contribute to uncorrelated events, as well as erroneous pairing of electrical and mechanical events. Finally, as we only focused on fasciculations, we do not know whether similar results would be obtained during voluntary muscle activation.

5. Conclusion

For the first time, this cross-sectional study combined MUS and HDSEMG simultaneously to assess the electromechanical properties of fasciculations in ALS. Our principal finding was an extended electromechanical latency from approximately 80 ms in healthy gastrocnemius muscles to approximately 110 ms in ALS biceps and gastrocnemius muscles. This result requires independent replication but points to an electromechanical defect within the muscles of ALS patients. In addition, HDSEMG was shown for the first time to reliably detect fasciculations as deep as 3 cm below the skin surface. Due to the high tolerance and accessibility of the two noninvasive techniques, this approach would be amenable to repeated measurements, providing robust comparisons with

established measures of disease progression. This could fuel novel therapy development in ALS by providing a quantifiable and easily applicable outcome measure in clinical drug trials.

Acknowledgements

JB acknowledges funding from the Medical Research Council and Motor Neurone Disease Assocation (Lady Edith Wolfson Clinical Research Training Fellowship; MR/P000983/1), Sattaripour Charitable Foundation, UK Dementia Research Institute and the National Institute for Health Research (Academic Clinical Lectureship program). DP, NM and CC contributed during their MSc qualifications in Clinical Neuroscience. R.I.'s input represents independent research supported by the NIHR BioResource Centre Maudsley at South London and Maudsley NHS Foundation Trust (SLaM) & Institute of Psychiatry, Psychology and Neuroscience (IoPPN), King's College London. We would like to thank all the patients involved in this study for their willingness and determination to participate. We thank TMSi for supplying the amplifier and sensors.

Appendix A. Supplementary material

Supplementary data to this article can be found online at https://doi.org/10.1016/j.clinph.2022.11.005.

References

Arts IM, Overeem S, Pillen S, Kleine BU, Boekestein WA, Zwarts MJ, Jurgen Schelhass H. Muscle ultrasonography: a diagnostic tool for amyotrophic lateral sclerosis. Clin Neurophysiol 2012;123:1662–7. https://doi.org/10.1016/j.clinph.2011.11.262.

Bashford J, Mills K, Shaw C. The evolving role of surface electromyography in amyotrophic lateral sclerosis: A systematic review. Clin Neurophysiol 2020a;131:942–50. https://doi.org/10.1016/j.clinph.2019.12.007.

Bashford J, Wickham A, Iniesta R, Drakakis E, Boutelle M, Mills K, Shaw CE. Preprocessing surface EMG data removes voluntary muscle activity and enhances SpiQE fasciculation analysis. Clin Neurophysiol 2020b;131:265–73. https://doi.org/10.1016/j.clinph.2019.09.015.

Bashford JA, Wickham A, Iniesta R, Drakakis EM, Boutelle MG, Mills KR, Shaw CE. The rise and fall of fasciculations in amyotrophic lateral sclerosis. Brain Commun 2020c;2. https://doi.org/10.1093/braincomms/fcaa018.

Bashford J, Wickham A, Iniesta R, Drakakis E, Boutelle M, Mills K, Shaw C. SpiQE: An automated analytical tool for detecting and characterising fasciculations in amyotrophic lateral sclerosis. Clin Neurophysiol 2019;130:1083–90. https://doi.org/10.1016/j.clinph.2019.03.032.

Benatar M, Boylan K, Jeromin A, Rutkove SB, Berry J, Atassi N, Bruijn L. ALS biomarkers for therapy development: State of the field and future directions. Muscle Nerve 2016;53:169–82. https://doi.org/10.1002/mus.24979.

Beqollari D, Romberg CF, Dobrowolny G, Martini M, Voss AA, Musaro A, Bannister RA. Progressive impairment of CaV1.1 function in the skeletal muscle of mice expressing a mutant type 1 Cu/Zn superoxide dismutase (G93A) linked to amyotrophic lateral sclerosis. Skelet Muscle 2016;6:24. https://doi.org/10.1186/s13395-016-0094-6.

Bibbings K, Harding PJ, Loram ID, Combres N, Hodson-Tole EF. Foreground Detection Analysis of Ultrasound Image Sequences Identifies Markers of Motor Neurone Disease across Diagnostically Relevant Skeletal Muscles. Ultrasound Med Biol 2019;45:1164–75. https://doi.org/10.1016/j.ultrasmedbio.2019.01.018.

Botter A, Vieira T, Carbonaro M, Cerone GL, Hodson-Tole EF. Electrodes' configuration influences the agreement between surface EMG and B-mode ultrasound detection of motor unit fasciculation. IEEE Access 2021;9:98100–20. https://doi.org/10.1109/ACCESS.2021.3094665.

Brooks BR, Miller RG, Swash M, Munsat TL. El Escorial revisited: revised criteria for the diagnosis of amyotrophic lateral sclerosis. Amyotroph Lateral Scler Other Motor Neuron Disord 2000;1:293–9. https://doi.org/10.1080/146608200300079536.

Longo DL, Brown RH, Al-Chalabi A. Amyotrophic Lateral Sclerosis. N Engl J Med 2017;377(2):162–72.

Calderon JC, Bolanos P, Caputo C. The excitation-contraction coupling mechanism in skeletal muscle. Biophys Rev 2014;6:133–60. https://doi.org/10.1007/s12551-013-0135-x.

Cedarbaum JM, Stambler N, Malta E, Fuller C, Hilt D, Thurmond B, Nakanishi A. The ALSFRS-R: a revised ALS functional rating scale that incorporates assessments of respiratory function. BDNF ALS Study Group (Phase III). J Neurol Sci 1999;169:13–21. https://doi.org/10.1016/s0022-510x(99)00210-5.

Chin ER, Chen D, Bobyk KD, Mazala DA. Perturbations in intracellular Ca2+ handling in skeletal muscle in the G93A*SOD1 mouse model of amyotrophic lateral sclerosis. Am J Physiol Cell Physiol 2014;307:C1031–8. https://doi.org/10.1152/ajpcell.00237.2013.

Dadon-Nachym M, Melamed E, Offen D. The "dying-back" phenomenon of motor neurons in ALS. J Mol Neurosci 2011;43:470–7. https://doi.org/10.1007/s12031-010-9467-1.

Daube JR, Rubin DI. Needle electromyography. Muscle Nerve 2009;39:244–70. https://doi.org/10.1002/mus.21180.

De Carvalho M, Kiernan MC, Swash M. Fasciculation in amyotrophic lateral sclerosis: origin and pathophysiological relevance. J Neurol Neurosurg Psychiatry 2017;88:773–9. https://doi.org/10.1136/jnnp-2017-315574.

De Carvalho M, Swash M. Lower motor neuron dysfunction in ALS. Clin Neurophysiol 2016;127:2670–81. https://doi.org/10.1016/j.clinph.2016.03.024.

Drost G, Kleine BU, Stegeman DF, Van Engelen BG, Zwarts MJ. Fasciculation potentials in high-density surface EMG. J Clin Neurophysiol 2007;24:301–7. https://doi.org/10.1097/WNP.0b013e31803bba04.

Duarte ML, Iared W, Oliveira ASB, Dos Santos LR, Peccin MS. Ultrasound versus electromyography for the detection of fasciculation in amyotrophic lateral sclerosis: systematic review and meta-analysis. Radiol Bras 2020;53:116–21. https://doi.org/10.1590/0100-3984.2019.0055.

Dyck PJ, Boes CJ, Mulder D, Millikan C, Windebank AJ, Dyck PJB, Espinosa R. History of standard scoring, notation, and summation of neuromuscular signs. A current survey and recommendation. J Peripher Nerv Syst 2005;10(2):158–73.

Feinstein B, Lindegard B, Nyman E, Wohlfart G. Morphologic studies of motor units in normal human muscles. Acta Anat (Basel) 1955;23:127–42. https://doi.org/10.1159/000140989.

Harding PJ, Loram ID, Combes N, Hodson-Tole EF. Ultrasound-Based Detection of Fasciculations in Healthy and Diseased Muscles. IEEE Trans Biomed Eng 2016;63:512–8. https://doi.org/10.1109/TBME.2015.2465168.

Hays RD, Sherbourne CD, Mazel RM. The RAND 36-Item Health Survey 1.0. Health Econ 1993;2:217–27. https://doi.org/10.1002/hec.4730020305.

Kaplan A, Spiller KJ, Towne C, Kanning KC, Choe GT, Geber A, Akay T, Aebischer P, Henderson CE. Neuronal matrix metalloproteinase-9 is a determinant of selective neurodegeneration. Neuron 2014;81:333–48. https://doi.org/10.1016/j.neuron.2013.12.009.

Kaewtrakulpong P, Bowden R. An improved adaptive background mixture model for realtime tracking with shadow detection. 2nd European Workshop on Advanced Video Based Surveillance Systems. Kluwer Academic; 2001. https://doi.org/10.1007/978-1-4615-0913-4_11.

Loram ID, Maganaris CN, Lakie M. Use of ultrasound to make noninvasive in vivo measurement of continuous changes in human muscle contractile length. J Appl Physiol 2006;1985(100):1311–23. https://doi.org/10.1152/japplphysiol.01229.2005.

Maimon R, Ionescu A, Bonnie A, Sweetat S, Wald-Altman S, Inbar S, Gradus T, Trotti D, Weil M, Behar O, Perlson E. miR126-5p Downregulation Facilitates Axon Degeneration and NMJ Disruption via a Non-Cell-Autonomous Mechanism in ALS. J Neurosci 2018;38:5478–94. https://doi.org/10.1523/JNEUROSCI.3037-17.2018.

Masrori P, Van Damme P. Amyotrophic lateral sclerosis: a clinical review. Eur J Neurol 2020;27:1918–29. https://doi.org/10.1111/ene.14393.

Mesin L, Farina D. A model for surface EMG generation in volume conductors with spherical inhomogeneities. IEEE Trans Biomed Eng 2005;52:1984–93. https://doi.org/10.1109/TBME.2005.857670.

Miguez D, Hodson-Tole EF, Loram I, Harding PJ. A technical note on variable inter-frame interval as a cause of non-physiological experimental artefacts in ultrasound. R Soc Open Sci 2017;4(5):170245.

Mills KR. Characteristics of fasciculations in amyotrophic lateral sclerosis and the benign fasciculation syndrome. Brain 2010;133:3458–69. https://doi.org/10.1093/brain/awq290.

Mills KR. The basics of electromyography. J Neurol Neurosurg Psychiatry 2005;76 (suppl_2):ii32–5.

Petrov D, Mansfield C, Moussy A, Hermine O. ALS Clinical Trials Review: 20 Years of Failure. Are We Any Closer to Registering a New Treatment? Front Aging Neurosci 2017;9:68. https://doi.org/10.3389/fnagi.2017.00068.

Pillen S, Arts IM, Zwarts MJ. Muscle ultrasound in neuromuscular disorders. Muscle Nerve 2008;37:679–93. https://doi.org/10.1002/mus.21015.

Riebe D, Franklin BA, Thompson PD, Garber CE, Whitfield GP, Magal M, Pescatello LS. Updating ACSM's Recommendations for Exercise Preparticipation Health Screening. Med Sci Sports Exerc 2015;47:2473–9. https://doi.org/10.1249/MSS.0000000000000664.

Tsuji Y, Noto Y-I, Shiga K, Teramukai S, Nakagawa M, Mizuno T. F48. A novel muscle ultrasound score in the diagnosis of amyotrophic lateral sclerosis. Clin Neurophysiol 2018;128:1069–74. https://doi.org/10.1016/j.clinph.2017.02.015.

Walker FO, Donofrio PD, Harpold GJ, Ferrell WG. Sonographic imagine of muscle contraction and fasciculations: a correlation with electromyography. Muscle Nerve 1990;13:33–9. https://doi.org/10.1002/mus.880130108.

Weddell T, Bashford J, Wickham A, Iniesta R, Chen M, Zhou P, Drakakis E, Boutelle M, Mills K, Shaw C. First-recruited motor units adopt a faster phenotype in amyotrophic lateral sclerosis. J Physiol 2021;599:4117–30. https://doi.org/10.1113/JP281310.

Zwarts MJ, Stegeman DF. Multichannel surface EMG: basic aspects and clinical utility. Muscle Nerve 2003;28:1–17. https://doi.org/10.1002/mus.10358.